Gate-controlled ballistic conductance of magnetic nanowires with double point contacts

V. Fallahi*

Department of Laser and Optical Engineering, University of Bonab, Bonab 5551761167, Iran

(Received 14 May 2017; published 2 August 2017)

Controlling the conductance and current flow through nanostructured magnetic point contacts is a key challenge for future spintronic devices. This could be achieved by exploiting the Rashba spin-orbit coupling effect induced by an external gate in the middle of two pinned domain walls at the point contacts. Here, I investigate the electrical conductance of a half-metallic diluted magnetic semiconductor nanowire with a double point contact exploitable in switching devices controlled by lateral gate voltage. The coherent quantum interference between forward- and backward-scattered waves in the spin quantum well formed by the double point contact leads to quasibound states with finite lifetimes. The energetic position of these quasibound states could be adjusted by the lateral gate voltage so that the incident energy coincides with one of the quasibound energy levels in the spin quantum well. Conductance calculations in the presence of an applied electric field perpendicular to the nanowire surface exhibit typical resonant tunneling behavior, where the nanostructure switches to the low-resistance ON state by tuning the Rashba coupling strength in the range of a few tens of meV nm. This study paves the way for utilizing the gate-controlled Rashba spin-orbit coupling effect to design and develop practical spintronic devices.

DOI: 10.1103/PhysRevB.96.064403

I. INTRODUCTION

The study of spin-dependent transport in ferromagnetic systems containing a domain wall has recently attracted much attention from both fundamental and technological viewpoints [1–12]. Special properties of the magnetic domain walls in controllable generation, manipulation, and detection of spin polarization have made them suitable candidates for memories [13] and logic devices [14]. In particular, narrow domain walls at sharp interfaces or point contacts have been the subject of many studies as the key components of the next generation spintronic devices, such as extremely high-density magnetic recording devices [15–18] and microwave oscillators [19]. Recent considerable interest in nanoscale domain walls geometrically trapped in point contacts stems from their ability to exhibit huge magnetoresistance (zero conductance) [20–29]. The huge magnetoresistance or so-called ballistic magnetoresistance (BMR) effect in point contacts can be explained by the large value of the nonadiabaticity parameter $\xi^{-1} \equiv \omega_{sd}\tau_W$ for narrow domain walls, in which $\omega_{sd} = \frac{\Delta_{ex}}{\hbar}$ is the angular frequency of the pseudo-Larmor precession of the electron spin about a rotating magnetic field that is determined by the $s-d$ exchange interaction energy Δ_{ex}, $\tau_W = \frac{2d}{v_F}$ refers to the time period of the wall magnetization rotation in the rest frame of an electron moving at the Fermi velocity v_F, and d denotes the wall thickness. The degree of nonadiabaticity could strongly be enhanced in the limit of weak exchange coupling ($\Delta_{ex} \to 0$) which is manifested in diluted magnetic semiconductors. Indeed, the ferromagnetism found in diluted magnetic semiconductors has opened up a completely new road to combine magnetism and charge transport in well-known semiconductor device structures. It is anticipated that the coupling between ferromagnetism and electronic transport in semiconductors would make the effect of magnetism significantly stronger than the corresponding phenomena observed in metals. Diluted magnetic semiconductors could exhibit half-metallic ferromagnetism, which presents ideally zero conductance (infinite magnetoresistance ratio) or 100% spin-polarized currents at the nanocontacts [30].

The conductance of a narrow domain wall pinned at the nanocontact can be reproducibly switched between "open" (zero conductance) and "closed" (nonzero conductance) states by changing a magnetic field applied perpendicular or parallel [31–33] to the wire axis. The dependence of the conductance on the angle of the magnetic field applied to the nanocontact has already been demonstrated by Shi *et al.* [34]. They argued that the modification of the contact configuration by changing the applied magnetic field could be responsible for abrupt steps in conductance. Switching the conductance of a half-metallic diluted magnetic semiconductor nanowire with a double point contact could be alternatively accomplished by controlling the distance between the point contacts as reported by Dugaev *et al.* [35]. Such a double-point-contact structure exhibits a resonant conductance, when the Fermi energy matches the resonant energy levels (quasibound states) of the spin quantum well formed between the point contacts [35,36]. Nevertheless, tuning the conductance by changing the distance between two point contacts is not practically possible since the point contacts are pinned at their positions. In this paper, I propose an alternative tuning technique based on the spin-orbit interaction induced by Rashba effect in a laterally gated spin quantum well. The energetic position of the quasibound states could be controlled by a lateral gate voltage applied between two magnetic point contacts. The dependence of the energy of these quasibound states on the Rashba spin-orbit coupling strength is employed to switch the conductance between ON and OFF states. In the following, the full quantum scattering theory is utilized to investigate the transmission probability through diluted magnetic semiconductor nanowire containing a double point contact. Then, the linear-response conductance is calculated in the presence of Rashba spin-orbit interaction induced by an external gate. Finally, a discussion of the results and conclusions is provided.

II. THEORETICAL CONSIDERATIONS

Full quantum scattering theory is utilized to investigate the conductance of a half-metallic ferromagnetic nanowire

*v.fallahi@bonabu.ac.ir

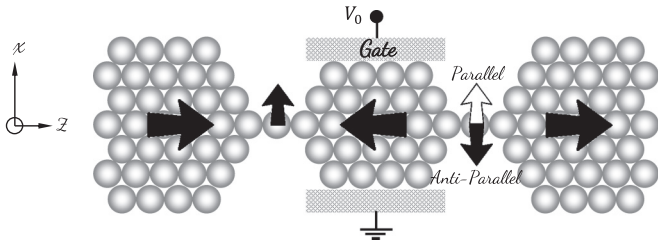

FIG. 1. The considered structure of two atomic-size domain walls between two semi-infinite nanowires with a lateral confinement potential, arising from the side gate in the system. The magnetizations of the domain walls could be configured in either parallel or antiparallel arrangements.

containing two atomic-size domain walls pinned at the nanocontacts. The general configuration of the two 180° head-to-head domain walls with lateral gate voltage applied between them is illustrated in Fig. 1. It is assumed that the magnetization direction depends only on the coordinate along the nanowire, i.e., the unit vector parallel to the local magnetization is defined by $\boldsymbol{m}(z) = [\sin\theta(z), 0, \cos\theta(z)]$, where $\theta(z)$ abruptly rotates counterclockwise from 0 to π at $z = -\frac{L}{2}$ and then makes a counterclockwise/clockwise jump from π to 2π at $z = +\frac{L}{2}$. The central section of the nanowire is subjected to the Rashba spin-orbit interaction brought about by an externally applied transverse electric field. The one-dimensional Hamiltonian of the system in the presence of the spin-orbit coupling interaction can be written as

$$H = \frac{p_z^2}{2m^*} - \Delta_{ex}\hat{\boldsymbol{\sigma}} \cdot \boldsymbol{m}(z) + \frac{\alpha(z)}{\hbar}\hat{\sigma}_y p_z, \tag{1}$$

where Δ_{ex} is the exchange integral, $\hat{\boldsymbol{\sigma}}$ denotes the spin operators in terms of the Pauli spin matrices, and $\alpha(z) = \alpha_0\Theta(z + \frac{L}{2})\Theta(\frac{L}{2} - z)$ is the Heaviside step function with Rashba coupling strength parameter (α_0). The Rashba spin-orbit coupling strength can be tuned by means of the lateral external gate voltage applied between two nanocontacts. In order to include a position-dependent Rashba field, the corresponding Hamiltonian can be symmetrized to result in a Hermitian operator as follows:

$$H_R = \frac{\alpha(z)}{\hbar}\hat{\sigma}_y p_z - \frac{i}{2}\alpha_0\hat{\sigma}_y\left\{\delta\left(z + \frac{L}{2}\right) - \delta\left(z - \frac{L}{2}\right)\right\}. \tag{2}$$

The last term in the above equation ensures that the current density is continuous across the interfaces. The full wave functions of an incident carrier with the Fermi energy ϵ_F in the left ($\mathcal{L}$), middle ($\mathcal{M}$), and right ($\mathcal{R}$) regions are

$$\Psi_{k,\sigma}^{(\mathcal{L})}(z) = I^{\uparrow}\begin{pmatrix}1\\0\end{pmatrix}e^{ik^{\uparrow}z} + r^{\uparrow}\begin{pmatrix}1\\0\end{pmatrix}e^{-ik^{\uparrow}z} + I^{\downarrow}\begin{pmatrix}0\\1\end{pmatrix}e^{ik^{\downarrow}z} + r^{\downarrow}\begin{pmatrix}0\\1\end{pmatrix}e^{-ik^{\downarrow}z}, \tag{3a}$$

$$\Psi_{k,\sigma}^{(\mathcal{M})}(z) = \frac{I^{+}}{\sqrt{1+\xi_+^2}}\begin{pmatrix}i\xi_+\\1\end{pmatrix}e^{ik_+z} + \frac{I^{-}}{\sqrt{1+\xi_-^2}}\begin{pmatrix}1\\-i\xi_-\end{pmatrix}e^{ik_-z} + \frac{R^{+}}{\sqrt{1+\xi_+^2}}\begin{pmatrix}-i\xi_+\\1\end{pmatrix}e^{-ik_+z} + \frac{R^{-}}{\sqrt{1+\xi_-^2}}\begin{pmatrix}1\\i\xi_-\end{pmatrix}e^{-ik_-z}, \tag{3b}$$

and

$$\Psi_{k,\sigma}^{(\mathcal{R})}(z) = t^{\uparrow}\begin{pmatrix}1\\0\end{pmatrix}e^{ik^{\uparrow}z} + t^{\downarrow}\begin{pmatrix}0\\1\end{pmatrix}e^{ik^{\downarrow}z}, \tag{3c}$$

in which $I^{\uparrow(\downarrow)}$ are the incoming up and down spin-wave intensities, $k^{\uparrow(\downarrow)} = \sqrt{k_F^2 \pm k_{ex}^2}$ represents the longitudinal wave vectors of the spin states at the Fermi surface, and $k_\pm^2 = k_F^2 + 2k_R^2 \pm \sqrt{k_{ex}^4 + 4k_F^2k_R^2 + 4k_R^4}$ denotes the wave vectors of the spin states in the middle region. The wave vectors k_F, k_{ex}, and k_R are defined as $k_F^2 = \frac{2m^*\epsilon_F}{\hbar^2}$, $k_{ex}^2 = \frac{2m^*\Delta_{ex}}{\hbar^2}$, and $k_R = \frac{m^*\alpha_0}{\hbar^2}$. The spin mistracking parameter is then given by $\xi_\pm = \frac{2k_\pm k_R}{k_\pm^2 - k_F^2 \pm k_{ex}^2}$. The coefficients $t^{\uparrow(\downarrow)}$ and $r^{\uparrow(\downarrow)}$ are the transmission and reflection amplitudes, respectively. The scattering states $\Psi_{k,\sigma}^{(\mathcal{L})}(z)$ and $\Psi_{k,\sigma}^{(\mathcal{R})}(z)$ describe the incoming spin waves from $z = -\infty$ to the right, which are partially reflected and partially transmitted into the two spin channels. In order to calculate the transmission amplitudes, I first assume the incoming wave to be entirely "up" and then consider a purely "down" spin state.

In the case of a sharp domain wall, i.e., $k_F d \ll 1$, one can consider the domain wall as a δ-like potential at $z = \pm\frac{L}{2}$ to calculate the transmission amplitudes. Regarding this δ-like potential, the first derivative of the scattering wave functions shows a discontinuity at $z = \pm\frac{L}{2}$. By integrating the Schrödinger equation over an infinitesimal region to span the δ-like potential at the nanocontacts, between $z = \pm\frac{L}{2} - \varepsilon$ and $z = \pm\frac{L}{2} + \varepsilon$ where $d \ll \varepsilon \ll k_F^{-1}$, one can find

$$\left.\frac{\partial\Psi_{k,\sigma}^{(\mathcal{M})}}{\partial z}\right|_{z=-\frac{L}{2}} = \left.\frac{\partial\Psi_{k,\sigma}^{(\mathcal{L})}}{\partial z}\right|_{z=-\frac{L}{2}} - \begin{pmatrix}0 & k_W^{\mathcal{L}} + k_R\\ k_W^{\mathcal{L}} - k_R & 0\end{pmatrix}\Psi_{k,\sigma}^{(\mathcal{L})}\Big|_{z=-\frac{L}{2}}$$

and

$$\left.\frac{\partial\Psi_{k,\sigma}^{(\mathcal{M})}}{\partial z}\right|_{z=+\frac{L}{2}} = \left.\frac{\partial\Psi_{k,\sigma}^{(\mathcal{R})}}{\partial z}\right|_{z=+\frac{L}{2}} + \begin{pmatrix}0 & k_W^{\mathcal{R}} - k_R\\ k_W^{\mathcal{R}} + k_R & 0\end{pmatrix}\Psi_{k,\sigma}^{(\mathcal{R})}\Big|_{z=+\frac{L}{2}},$$

in which $k_W^{\mathcal{R}(\mathcal{L})} = \frac{2m^*\Delta_{ex}}{\hbar^2}\int_{\pm\frac{L}{2}-\varepsilon}^{\pm\frac{L}{2}+\varepsilon}\sin\theta(z)dz$, which could be defined as the spin-flip wave vector transfer. Then, the transmission and reflection amplitudes are obtained by matching the continuity of the spin-wave functions and the above discontinuity relations at the interfaces.

The transmission coefficients are evaluated as the ratio of the transmitted to the incident probability current density. The

probability current density is calculated using the following form in the presence of the spin-orbit coupling tuned by a gate voltage:

$$\mathcal{J} = \frac{1}{m*}\mathrm{Re}\{\langle\Psi|p_z + \hbar k_R(z)\sigma_y|\Psi\rangle\}, \quad (4)$$

and subsequently, the transmission coefficients will be obtained as follows:

$$T^{pq} = \frac{\mathcal{J}_t^q}{\mathcal{J}_i^p}\Xi(k^p)\Xi(k^q), \;\; p,q = \uparrow \text{ and } \downarrow, \quad (5)$$

in which $\mathcal{J}_i^{\uparrow(\downarrow)}$ and $\mathcal{J}_t^{\uparrow(\downarrow)}$ are incident and transmitted probability current densities for up and down spin states, respectively. Then, the total transmission coefficients for the incoming up and down spin states will be equal to $T^{\uparrow} = T^{\uparrow\uparrow} + T^{\uparrow\downarrow}$ and $T^{\downarrow} = T^{\downarrow\uparrow} + T^{\downarrow\downarrow}$, respectively. The Heaviside function $\Xi(k^{\uparrow(\downarrow)})$ is considered in order to eliminate evanescent spin-wave functions. In this way, $\Xi(k^{\uparrow(\downarrow)})$ will be equal to zero in the case of $\mathrm{Im}(k^{\uparrow(\downarrow)}) \neq 0$.

Assuming that the incoming electronic spin is an unpolarized statistical mixture, i.e., $\rho_{in} = \frac{1}{2}(|\uparrow\rangle\langle\uparrow| + |\downarrow\rangle\langle\downarrow|)$, the output will be obtained by $\rho_{\text{out}} = \frac{1}{2}[(T^{\uparrow\downarrow} + T^{\downarrow\downarrow})|\uparrow\rangle\langle\uparrow| + (T^{\downarrow\uparrow} + T^{\uparrow\uparrow})|\downarrow\rangle\langle\downarrow|]$ [37]. Therefore, the overall transmission coefficient of the unpolarized electrons will be given by $T = \frac{1}{2}(T^{\uparrow} + T^{\downarrow})$. In the case reported here, it is not taken into account the possibility that electrons could be partially polarized before ballistic transport through the ferromagnetic material is not taken into account.

At low bias voltage, the domain-wall conductance is calculated according to the Landauer-Büttiker formalism [38]. This approach, which is widely used in mesoscopic physics, expresses the conductance in terms of the transmission properties of coherent electron states as follows:

$$\mathcal{G} = \frac{2e^2}{h}T. \quad (6)$$

So, the MR can be calculated using the following relation:

$$\frac{\delta\rho}{\rho_0} = -\frac{\delta\mathcal{G}}{\mathcal{G}} = \frac{\mathcal{G}_0}{\mathcal{G}} - 1, \quad (7)$$

in which $\rho_0 = \mathcal{G}_0^{-1}$ and $\mathcal{G}_0 = \frac{2e^2}{h}(\frac{\Xi(k^{\uparrow})+\Xi(k^{\downarrow})}{2})$ is the conductance of the nanowire without the domain wall.

III. RESULTS AND DISCUSSION

In the calculations, I considered a diluted magnetic semiconductor $Ga_{1-x}Mn_xAs$ nanowire consisting of a double sharp domain wall separated by a distance L. The ferromagnetic semiconductors $Ga_{1-x}Mn_xAs$ with typical spin splitting energy $\Delta_{ex} = 50$ meV [39], and the valence hole effective mass $m = 0.47$ (in units of the free electron mass m_0) can exhibit half-metallic ferromagnetic behavior with 100% spin-polarized currents at the Fermi level $2m\epsilon_F = (3\pi^2\hbar^3 p)^{2/3}$ for the hole concentration $p \leqslant 1.65 \times 10^{19}\,\mathrm{cm}^{-3}$. In this case, $\epsilon_F < \Delta_{ex}$, the incoming minority spin would have a negative kinetic energy and transmission is blocked in ferromagnetic regions [40]. Instead, the holes in the majority spin states are able to tunnel through the potential barrier formed between two magnetic domain walls.

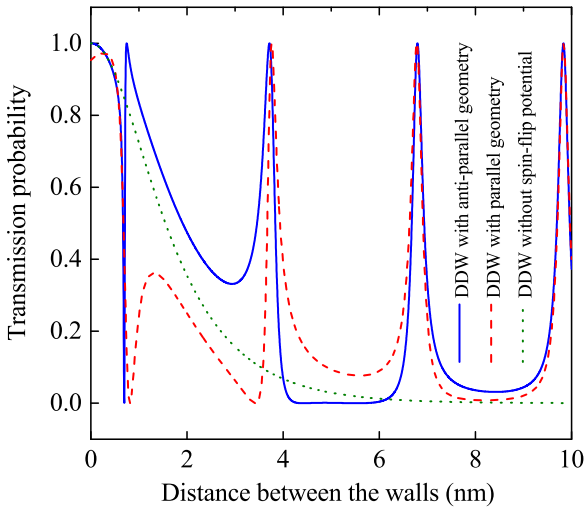

FIG. 2. The transmission probability through a double domain wall plotted as a function of the separation distance between two domain walls L in the presence of the spin-flip potential for the cases where the magnetizations of the two domain walls are antiparallel (solid line), parallel (dashed line), and in the absence of the spin-flip potential (dotted line). The parameters used in the calculations are $d = 0.5$ nm, $\Delta_{ex} = 50$ meV, $p = 1 \times 10^{19}\,\mathrm{cm}^{-3}$, and $\alpha_0 = 0$. The resonance peaks for the parallel and antiparallel aligned structures coincide with each other at larger distances.

The dependence of the transmission probability on the domain-wall separation distance is shown in Fig. 2 for parallel and antiparallel aligned magnetic nanocontacts. The probability of transmission in the absence of the spin-flip potential is also depicted for more qualitative discussion. As can be seen, in the limit $L \to 0$, the incoming holes from the left lead can pass through the structure without any scattering in the antiparallel case where the two opposing spin-flip potentials cancel each other out, while they experience reflection by the nonzero effective spin-flip potential in the parallel aligned domain walls. In the absence of the spin-flip mechanism, the majority carriers traveling through a sharp domain wall cannot change their spin orientation and hence are effectively reflected from the exchange potential barrier. In this case, the majority spin holes in the left lead actually become the minority holes in the middle ferromagnetic region that they would not be allowed to transmit, so transport of holes would occur through nonresonant tunneling. It should be noted that the exchange potential becomes zero in the limit $L \to 0$, and unity transmission is obtained. On the other hand, the majority spin holes that experience spin-flip scattering in transmission through the first domain wall remain the majority spin holes that propagate in the middle ferromagnetic region and would be either reflected or transmitted at the interfaces. As a result, a set of the plane-wave functions is formed that would be transmitted back into the left lead, resulting in either constructive or destructive interference. The degree to which these wave functions can cancel each other out is determined by the separation distance between the two domain walls. For some values of L, the interference is completely destructive, so the unity transmission corresponding to resonant tunneling is obtained. The resonance peaks corresponding to those values

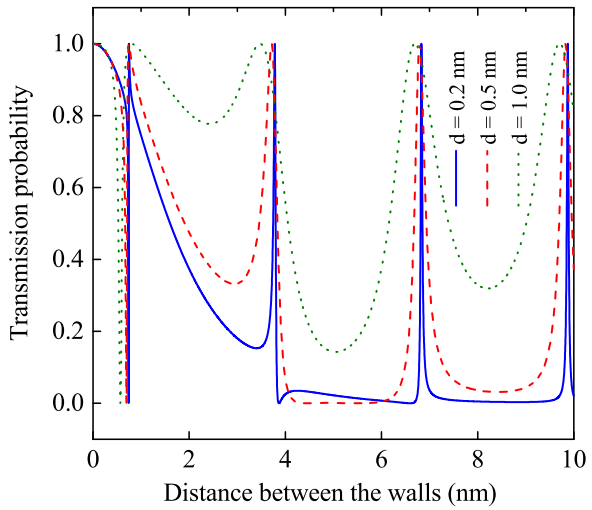

FIG. 3. The transmission probability through a double domain wall with antiparallel configuration plotted as a function of the separation distance L between two domain walls for different values of the domain-wall thickness d. The other parameters are as in Fig. 2.

of L for which $r^{\uparrow} = \pm t^{\uparrow}$ are spaced approximately $\Delta L \cong \frac{n\pi}{k^{\uparrow}}$ apart, which is the same as the Bragg condition in a periodic medium.

The transmission probability as a function of L for different values of the domain-wall thickness d is also depicted in Fig. 3. It reveals a slight shift and broadening of the resonance peaks with increasing the domain-wall thickness. Thick domain walls exhibit smooth spin-flip potentials at which adiabatic spin-flip scattering would take place. The adiabatic spin-flip transition facilitates carrier tunneling and leads to broadening of the transmission resonance peaks. Also, spatial spread of the exchange potential by the domain-wall thickness contributes to the peak shift.

The quantum confinement of the spin-down holes (majority spins of the middle region) in the double-domain-wall structure leads to the formation of discrete energy levels in the energy range $\epsilon \equiv [-11]\Delta_{ex}$. It is found that the resonant transmissions are associated with the excitation of these quasibound states localized in the finite exchange potential well, or so-called spin quantum well. The spin-down quantum levels are coupled to the continuous energy levels of the leads via spin-flip transmission and reflection amplitudes, namely, $t^{\uparrow}$ and $r^{\uparrow}$. A possible escape to the leads is responsible for the broadening of these quasibound levels and hence a finite lifetime (τ), which is determined by the spin-mixing parameter $\Lambda^{\mathcal{L}(\mathcal{R})} = k_W^{\mathcal{L}(\mathcal{R})} d$ for the domain walls residing in the nanocontacts. The energetic position of these quasibound states as well as their finite lifetimes can be calculated from the probability of tunneling through the spin quantum well. Figure 4 shows the contour plot of the transmission probability as a function of incident energy ϵ_F and separation distance L for different gate bias voltages. The logarithm of the transmission probability versus incident energy ϵ_F is plotted in the right panels of Fig. 4 for spin-up carriers traveling through the double-domain-wall structure with antiparallel configuration for $L = 5,10$ nm.

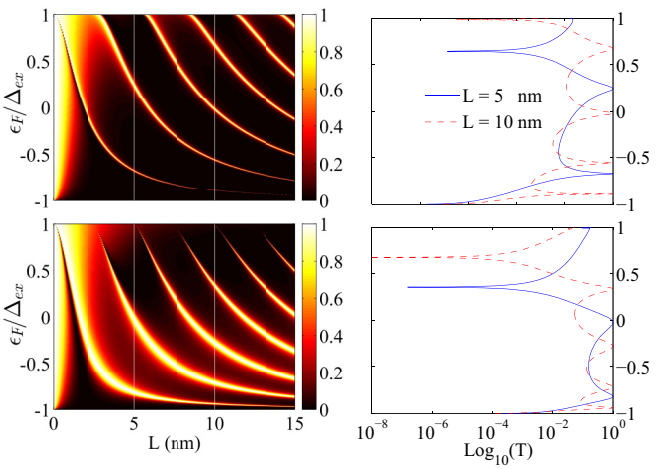

FIG. 4. Left panels: Contour plot of the transmission probability as a function of the incident energy ϵ_F and separation distance L for different lateral gate bias voltages corresponding to the Rashba parameters $\alpha_0 = 0$ meV nm (upper) and $\alpha_0 = 50$ meV nm (lower). Right panels: The logarithm of the transmission probability through the double-domain-wall structure as a function of energy for fixed separation distances $L = 5$ nm and $L = 10$ nm. The domain-wall thickness is $d = 0.5$ nm, and the spin splitting energy and the hole density are $\Delta_{ex} = 50$ meV and $p = 1 \times 10^{19}$ cm^{-3}, respectively.

At near-zero biasing voltage, the broadening of the resonance peaks at high energy levels is clearly observed, which can be demonstrated by the fact that the higher localized states leak rapidly out of the middle region into the leads. Obviously, at the finite Rashba coupling strength, the transmission peaks show a broadening and redshift (toward lower energy). It should be pointed out that applying the lateral gate voltage tunes the Rashba spin-orbit coupling strength in consistence with the well-known relation between α_0 and average electric field $E = -\langle \partial V/\partial x \rangle$: $\alpha_0 = e\gamma_R \langle \partial V/\partial x \rangle$. It has been shown that the average value of intrinsic surface potential gradient $\langle \partial V/\partial x \rangle$ is of the order of 1mV/Å [41]. Taking into account

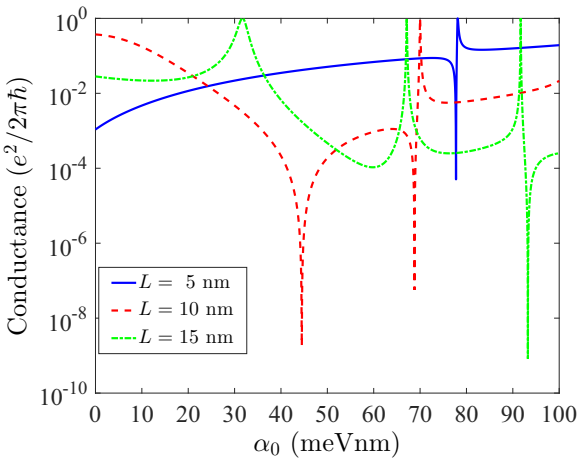

FIG. 5. Logarithmic conductance of the double-domain-wall structure as a function of the Rashba spin-orbit coupling strength for the domain-wall separation distances $L = 5$ nm, $L = 10$ nm, and $L = 15$ nm.

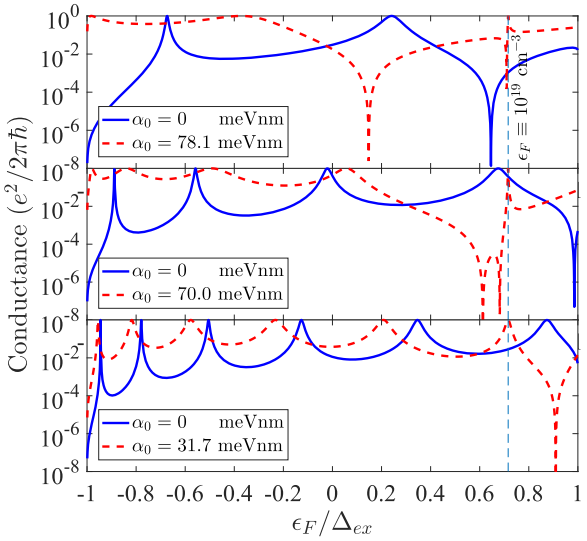

FIG. 6. Logarithmic conductance of the double-domain-wall structure as a function of Fermi energy for the domain-wall separation distances $L = 5$ nm (top), $L = 10$ nm (middle), and $L = 15$ nm (bottom). Resonance peaks for two antiparallel sharp magnetic domain walls in the presence of the Rashba spin-orbit interaction are shifted to lower energies.

the $\gamma_R = 5 - 500\text{Å}^2$ for III-V semiconductors [42], the value of the intrinsic Rashba strength can vary in the range of a few meV nm to a few tens of meV nm. On the other hand, tuning the Rashba spin-orbit coupling strength is also possible via biasing with a top gate. It has been demonstrated that the Rashba coupling strength can be enhanced up to 50% by the gate field [43]. In particular, electrolyte gating with only 1 V of gate bias voltage could make the Rashba coefficient 6 times larger [44]. Using the lowest value for γ_R, the data in Fig. 4 (lower panels) correspond to the highest value for $E \approx 10$ MV/cm, experimentally generated at the surface of the nanowire in the electrolyte gating. The gate-controlled Rashba spin-orbit interaction would induce spin precession of the hole tunneling through the spin quantum well with a spin-dependent phase shift $\Delta\varphi = \pm k_R L$. This phase shift is responsible for the modulation of the quantum interference at the well boundaries that would change the energetic positions of the quasibound levels in the resonant tunneling. Moreover, the spatial discontinuity of the Rashba spin-orbit coupling imposes an additional spin-flip wave-vector transfer $\pm k_R$ to the majority (minority) carriers impinging on the walls at the nanocontacts. Indeed, the Rashba spin-orbit interaction manipulates the spin-mixing parameter as $\Lambda^{\mathcal{L}(\mathcal{R})} = d(k_W^{\mathcal{L}(\mathcal{R})} \pm k_R)$ for the incoming majority (minority) carriers in the antiparallel aligned domain walls. As a consequence, the spin-mixing parameter increases as a function of the lateral gate voltage for pure spin-up incident holes and thus broadens the resonance peaks of the transmission.

According to the Landauer-Büttiker formula, the ballistic conductance $\mathcal{G}$ is related to the transmission probability T at the Fermi energy in the linear-response regime. The conductance of the double-domain-wall structure is shown in Fig. 5 as a function of the Rashba spin-orbit coupling strength. As shown, the first sharp resonant peak of the conductance shifts toward the lower values of the Rashba parameter as the separation distance between two nanocontacts increases. For a given double-domain-wall structure with parameters $d = 0.5$ nm, $p = 1 \times 10^{19}$ cm^{-3}, and $\Delta_{ex} = 50$ meV, the conductance curves show two sharp resonance peaks at points $\alpha_0 \approx 78$ meV nm, $\alpha_0 \approx 70$ meV nm and $\alpha_0 \approx 31.7$ meV nm for domain-wall separation distances $L = 5$ nm, $L = 10$ nm, and $L = 15$ nm, respectively. As can be seen in Fig. 6, these points correspond to those values of Rashba coupling strength that push the energetic position of the quasibound states downwards until one of them coincides with the Fermi energy.

IV. CONCLUSION

In summary, the influence of the gate-controlled Rashba spin-orbit coupling on the tunneling conductance of a half-metallic magnetic semiconductor nanowire which contains a double point contact has been investigated in the ballistic regime. The quantum confinement of the holes between two pinned domain walls at the point contacts leads to the formation of the quasibound states. The resonance peaks in the transmission probability as well as the conductance spectrum have been observed near the energies of the quasibound states. It has been shown that the spin precession of the hole tunneling through the spin quantum well could be controlled by the lateral gate voltage or the electric field via the effective magnetic field generated by the Rashba spin-orbit interaction. It has been found that the induced phase shift due to the Rashba spin-orbit interaction is responsible for the modulation of the quantum interference at the well boundaries that would change the energetic positions of the quasibound levels in the resonant tunneling. Furthermore, the spin-mixing parameter which determines the lifetime of the quasibound states is changed due to the spatial discontinuity of the Rashba spin-orbit interaction at the well boundaries. Such findings highlight the potential use of lateral gate voltage to switch the conductance of a double-point-contact device as an active component of new spintronic devices.

[1] P. M. Levy and S. Zhang, Phys. Rev. Lett. **79**, 5110 (1997).
[2] A. Brataas, G. Tatara, and G. E. W. Bauer, Phys. Rev. B **60**, 3406 (1999).
[3] U. Ebels, A. Radulescu, Y. Henry, L. Piraux, and K. Ounadjela, Phys. Rev. Lett. **84**, 983 (2000).
[4] V. K. Dugaev, J. Barnaś, A. Łusakowski, and L. A. Turski, Phys. Rev. B **65**, 224419 (2002).
[5] V. K. Dugaev, J. Berakdar, and J. Barnaś, Phys. Rev. B **68**, 104434 (2003).
[6] V. K. Dugaev, J. Barnaś, J. Berakdar, V. I. Ivanov, W. Dobrowolski, and V. F. Mitin, Phys. Rev. B **71**, 024430 (2005).

[7] E. Šimánek and A. Rebei, Phys. Rev. B **71**, 172405 (2005).
[8] M. Ghanaatshoar, V. Fallahi, M. M. Tehranchi, and A. Phirouznia, IEEE Trans. Magn. **44**, 3127 (2008).
[9] A. Phirouznia, M. M. Tehranchi, and M. Ghanaatshoar, Phys. Rev. B **75**, 224403 (2007).
[10] V. Fallahi and M. Ghanaatshoar, Phys. Rev. B **82**, 035210 (2010).
[11] E. A. Golovatski and M. E. Flatté, Phys. Rev. B **84**, 115210 (2011).
[12] S. Allende, J. Retamal, D. Altbir, and J. d'Albuquerque e Castro, J. Magn. Magn. Mater. **355**, 197 (2014).
[13] S. S. P. Parkin, M. Hayashi, and L. Thomas, Science **320**, 190 (2008).
[14] D. A. Allwood, G. Xiong, C. C. Faulkner, D. Atkinson, D. Petit, and R. P. Cowburn, Science **309**, 1688 (2005).
[15] P. Bruno, Phys. Rev. Lett. **83**, 2425 (1999).
[16] N. García, M. Muñoz, G. G. Qian, H. Rohrer, I. G. Saveliev, and Y. W. Zhao, Appl. Phys. Lett. **79**, 4550 (2001).
[17] M. Muñoz, G. G. Qian, N. Karar, H. Cheng, I. G. Saveliev, N. García, T. P. Moffat, P. J. Chen, L. Gan, and W. F. Egelhoff, Appl. Phys. Lett. **79**, 2946 (2001).
[18] A. R. Rocha and S. Sanvito, Phys. Rev. B **70**, 094406 (2004).
[19] H. Suzuki, H. Endo, T. Nakamura, T. Tanaka, M. Doi, S. Hashimoto, H. N. Fuke, M. Takagishi, H. Iwasaki, and M. Sahashi, J. Appl. Phys. **105**, 07D124 (2009).
[20] V. Fallahi and R. Safaei, Phys. Rev. B **94**, 064426 (2016).
[21] H. D. Chopra and S. Z. Hua, Phys. Rev. B **66**, 020403 (2002).
[22] W. F. Egelhoff, L. Gan, H. Ettedgui, Y. Kadmon, C. J. Powell, P. J. Chen, A. J. Shapiro, R. D. McMichael, J. J. Mallett, T. P. Moffat *et al.*, J. Appl. Phys. **95**, 7554 (2004).
[23] V. Fallahi, J. Supercond. Novel Magn. (2017), URL http://dx.doi.org/10.1007/s10948-017-4073-x.
[24] H. D. Chopra, M. R. Sullivan, J. N. Armstrong, and S. Z. Hua, Nat. Mater. **4**, 832 (2005).
[25] M. R. Sullivan, D. A. Boehm, D. A. Ateya, S. Z. Hua, and H. D. Chopra, Phys. Rev. B **71**, 024412 (2005).
[26] N. Useinov and L. Tagirov, J. Magn. Magn. Mater. **321**, 3246 (2009).
[27] V. Fallahi and M. Ghanaatshoar, Eur. Phys. J. B **80**, 401 (2011).
[28] V. Fallahi and M. Ghanaatshoar, Phys. Status Solidi B **249**, 1077 (2012).
[29] A. von Bieren, A. K. Patra, S. Krzyk, J. Rhensius, R. M. Reeve, L. J. Heyderman, R. Hoffmann-Vogel, and M. Kläui, Phys. Rev. Lett. **110**, 067203 (2013).
[30] S. A. Wolf, D. D. Awschalom, R. A. Buhrman, J. M. Daughton, S. von Molnár, M. L. Roukes, A. Y. Chtchelkanova, and D. M. Treger, Science **294**, 1488 (2001).
[31] M. Müller, R. Montbrun, M. Marz, V. Fritsch, C. Sürgers, and H. V. Löhneysen, Nano Lett. **11**, 574 (2011).
[32] S. N. Jammalamadaka, S. Kuntz, O. Berg, W. Kittler, U. M. Kannan, J. A. Chelvane, and C. Sürgers, Sci. Rep. **5** (2015).
[33] U. M. Kannan, S. Kuntz, O. Berg, W. Kittler, H. Basumatary, J. A. Chelvane, C. Sürgers, and S. N. Jammalamadaka, Appl. Phys. Lett. **108**, 242408 (2016).
[34] S. F. Shi, K. I. Bolotin, F. Kuemmeth, and D. C. Ralph, Phys. Rev. B **76**, 184438 (2007).
[35] V. K. Dugaev, J. Berakdar, and J. Barnaś, Phys. Rev. Lett. **96**, 047208 (2006).
[36] R. Zhu and J. Berakdar, Phys. Rev. B **81**, 014403 (2010).
[37] V. M. Ramaglia, D. Bercioux, V. Cataudella, G. D. Filippis, and C. A. Perroni, J. Phys.: Condens. Matter **16**, 9143 (2004).
[38] M. Lundstrom, *Fundamentals of Carrier Transport* (Cambridge University Press, Cambridge, UK, 2009).
[39] H. Ohno, N. Akiba, F. Matsukura, A. Shen, K. Ohtani, and Y. Ohno, Appl. Phys. Lett. **73**, 363 (1998).
[40] V. A. Gopar, D. Weinmann, R. A. Jalabert, and R. L. Stamps, Phys. Rev. B **69**, 014426 (2004).
[41] C. L. Romano, S. E. Ulloa, and P. I. Tamborenea, Phys. Rev. B **71**, 035336 (2005).
[42] R. de Sousa and S. Das Sarma, Phys. Rev. B **68**, 155330 (2003).
[43] J. B. Miller, D. M. Zumbühl, C. M. Marcus, Y. B. Lyanda-Geller, D. Goldhaber-Gordon, K. Campman, and A. C. Gossard, Phys. Rev. Lett. **90**, 076807 (2003).
[44] D. Liang and X. P. Gao, Nano Lett. **12**, 3263 (2012).